



TITLE:

# Optimal Experimental Condition of IR pMAIRS Calibrated by Using an Optically Isotropic Thin Film Exhibiting the Berreman Effect

AUTHOR(S):

Shioya, Nobutaka; Norimoto, Shingo; Izumi, Naoki; Hada, Miyako; Shimoaka, Takafumi; Hasegawa, Takeshi

---

CITATION:

Shioya, Nobutaka ...[et al]. Optimal Experimental Condition of IR pMAIRS Calibrated by Using an Optically Isotropic Thin Film Exhibiting the Berreman Effect. Applied Spectroscopy 2017, 71(5): 901-910

ISSUE DATE:

2017-05

URL:

<http://hdl.handle.net/2433/224993>

RIGHT:

The final, definitive version of this paper has been published in 'Applied Spectroscopy, Vol. 71(5) 901-910' by SAGE Publications Ltd, All rights reserved. © The Authors.; This is not the published version. Please cite only the published version.; この論文は出版社版ではありません。引用の際には出版社版をご確認ご利用ください。

# Optimal Experimental Condition of IR pMAIRS Calibrated by Using an Optically Isotropic Thin Film Exhibiting the Berreman Effect

*Nobutaka Shioya, Shingo Norimoto, Naoki Izumi, Miyako Hada, Takafumi Shimoaka,*

*and Takeshi Hasegawa<sup>†</sup>*

Laboratory of Solution and Interface Chemistry, Division of Environmental Chemistry,  
Institute for Chemical Research, Kyoto University, Gokasho, Uji, Kyoto 611-0011,  
Japan

<sup>†</sup> Author to whom correspondence should be addressed.

[htakeshi@scl.kyoto-u.ac.jp](mailto:htakeshi@scl.kyoto-u.ac.jp)

FAX: +81 778-38-3074

The present address:

Shingo Norimoto: JASCO Co. Ltd., Ishikawa-machi, Hachioji, Tokyo 192-8537, Japan

**Abstract:** IR p-polarized multiple-angle incidence spectrometry (pMAIRS) is a useful spectroscopic tool for revealing the molecular anisotropic structure in a thin film, which is used for the molecular orientation analysis of many functionalized organic thin films. IR pMAIRS provides both in-plane (IP) and out-of-plane (OP) vibrational mode spectra, which are influenced by the choice of the angles of incidence, i.e., angle set. To obtain quantitatively reliable pMAIRS spectra, therefore, the optimal angle set must be revealed. In a former study, an optimization study was carried out on a silicon substrate by using the band intensity ratio of the IP and OP spectra of highly oriented molecules in a thin film, which has a problem that the optimized results cannot be used for another substrate. In the present study, a totally new idea using an optically isotropic thin film as a standard sample is proposed to comprehensively explore the optimal angle set on various substrates: the band shift due to the Berreman effect of a strongly absorbing compound is used, instead of the band intensity. This new approach makes the pMAIRS calibration for various substrates a much easier task. With the optimal angle set, the molecular orientation angle in the film calculated by the pMAIRS spectra is also found to be reliable quantitatively. This technique opens a user-friendly way to a reliable molecular orientation analysis in an ultrathin film using IR pMAIRS.

**Keywords:** IR pMAIRS, Berreman effect, TO-LO splitting, Standard sample, Molecular orientation

## Introduction:

Infrared multiple-angle incidence resolution spectrometry (IR MAIRS)<sup>1,2</sup> is a powerful spectroscopic tool for revealing the molecular anisotropic structure in an organic thin film.<sup>3,4</sup> This spectroscopic technique provides both in-plane (IP) and out-of-plane (OP) spectra, which reveals the surface-parallel ( $x$ ) and -perpendicular ( $z$ ) components of a transition moment, respectively, at a time from an identical sample. Since both  $x$  and  $z$  components are available for every absorption band, IR MAIRS makes the molecular orientation analysis of each chemical group an easy task irrespective of the degree of crystallinity of the thin film.

The original MAIRS technique that employs an un-polarized IR light has an experimental limitation that a low refractive-index substrate such as  $\text{CaF}_2$  and glass cannot be used as the substrate. This problem is readily overcome by employing of an advanced technique, pMAIRS,<sup>5</sup> which employs the p-polarization. In both techniques, the spectra are influenced by the experimental parameters,<sup>6,7</sup> particularly by the choice of the angles of incidence.<sup>7</sup> If inappropriate angles are chosen, inaccurate results are yielded.<sup>7</sup>

To quantitatively discuss MAIRS (or pMAIRS) spectra, an expression deduced from Maxwell equations by Itoh et al. is quite useful (Eq. 1).<sup>8</sup>



$$\begin{aligned} A_{\text{IP}} &= \frac{8\pi d_2}{\lambda} \left[ h_{\text{x}}^{\text{IP}} \text{Im}(\varepsilon_{\text{x}}) + h_{\text{z}}^{\text{IP}} \text{Im}\left(-\frac{1}{\varepsilon_{\text{z}}}\right) \right] \\ A_{\text{OP}} &= \frac{8\pi d_2}{\lambda} \left[ h_{\text{x}}^{\text{OP}} \text{Im}(\varepsilon_{\text{x}}) + h_{\text{z}}^{\text{OP}} \text{Im}\left(-\frac{1}{\varepsilon_{\text{z}}}\right) \right] \end{aligned} \quad (1)$$

Here,  $A_{\text{IP}}$  and  $A_{\text{OP}}$  represent the IP and OP spectra, respectively, each of which is a linear combination of  $\text{Im}(\varepsilon_{\text{x}})$  and  $\text{Im}(-1/\varepsilon_{\text{z}})$  that are called transverse and longitudinal optic (TO and LO) energy-loss functions, respectively (Figure 1), involving the  $x$ - and  $z$ -components (surface-parallel and -perpendicular, respectively) of the electric permittivity,  $\varepsilon$ , of the thin film.<sup>9</sup> The rest parameters of  $\lambda$  and  $d_2$  are the wavelength at a band, and the film thickness, respectively. The TO and LO functions are used for theorizing the conventional transmission and reflection-absorption (RA) spectra, respectively (Figure 1).<sup>9,10</sup> In addition, the weighting factors of  $h_{\text{x}}^{\text{IP}}$ ,  $h_{\text{z}}^{\text{IP}}$ ,  $h_{\text{x}}^{\text{OP}}$  and  $h_{\text{z}}^{\text{OP}}$  depend on other parameters of the polarization purity, the refractive index of the substrate and the angles of incidence. This means that no parameter of the analyte film is, fortunately, needed for the calculation of the weighting factors. Here, the optimal angles of incidence involve the starting angle, the ending angle and the number of measurement points, which is called “angle set” throughout this paper.

When the optimal angle set is chosen, MAIRS-IP and -OP spectra should

correspond to the TO and LO functions, respectively, (Figure 1). This implies that the weighting factor for the LO function involved in the IP spectrum,  $h_z^{\text{IP}}$ , must be nearly zero to leave an accurate MAIRS-IP spectrum only. In a similar manner, for the OP spectrum, the contribution of the TO function ( $h_x^{\text{OP}}$ ) must be close to zero. In this manner, the accurate IP and OP spectra can be measured only when the optimal angle set is chosen to make the factors nearly zero. In other words, by choosing the optimal angle set, the molecular orientation can be discussed without a priori knowledge of optical constants, which is a significant benefit of using IR pMAIRS as compared to other analytical techniques.<sup>10,11</sup>

The optimal angle set, however, has not been studied in a comprehensive manner thus far. The empirically determined condition on a single example induces confusion that the angle set can commonly be employed for some substrates. Nagao studied<sup>12,13</sup> a functionalized polymer thin film prepared on some substrates using the IR pMAIRS technique with an angle set of 6 angles from 8° to 38° by 6° steps ( $38^\circ = 8^\circ + 6^\circ \times 5$ ), which readily revealed chemically new insights. Since the angle set for calibrating MAIRS was determined on a single sample, however, the optimization does not look over a wide variety of substrates with various refractive indices.

What is worse, there has been no standard sample to calibrate the MAIRS (or

pMAIRS) spectra. Since the MAIRS spectra give an image of molecular orientation, the standard sample has long been believed to have oriented molecules. Therefore, a Langmuir-Blodgett (LB) film and a self-assembled monolayer (SAM) were employed as a good candidate.<sup>6,7</sup> Nevertheless, LB films and SAMs are generally difficult to prepare, and the molecular orientation analysis in the samples needs another technique, such as X-ray diffraction etc, to make the samples a good standard.<sup>1,7</sup>

To get over the many practical difficulties about the MAIRS technique, in the present study, a totally new concept is proposed using an ‘isotropic’ standard sample to calibrate IR MAIRS. In place of discussing the band intensity ratio of the IP and OP spectra, Berreman’s effect<sup>14</sup> is focused on. Berreman’s effect, which is known as the TO-LO splitting,<sup>15,16</sup> gives a band shift induced by a large dispersion of the real part of the complex refractive index, which occurs when the imaginary part is very large (strong absorption).

As the strongly absorbing material, a perfluoroalkyl (Rf) compound is quite suitable. Since the C–F bond has a large permanent dipole moment, the C–F stretching vibration band exhibits a very large absorbance, which induces a large band shift via Berreman’s effect.<sup>16-18</sup> Since the band positions due to the TO-LO splitting can accurately be calculated from the spectrum of an isotropic sample, a standard sample

having an isotropic structure is preferable. To satisfy these conditions, poly(2-perfluorobutylethyl acrylate) (C4FA; Chart 1) is employed. In the present study, only the pMAIRS technique is optimized, since pMAIRS exhibits a much better performance than the original MAIRS as mentioned later.

C4FA is a gel-like liquid because of a short Rf side chain,<sup>17,19</sup> and thus an isotropic film ( $\varepsilon_x = \varepsilon_y = \varepsilon_z$ ) can easily be prepared by spreading the sample on a solid substrate.<sup>19</sup> The ideal pMAIRS-IP and -OP spectra are readily predicted by using Kramers-Kronig's (KK) relationship from an attenuated total reflection (ATR) spectrum of a bulk sample of C4FA (Figure 1). If the optimal angle set is chosen, the measured pMAIRS spectra would agree with the calculated prediction ( $A_{IP} \propto \text{To function}$ ;  $A_{OP} \propto \text{LO function}$ ). Fortunately, the optimal angle set has readily been obtained for representative IR-transparent substrates, which enables us to employ IR pMAIRS technique for quantitative analysis of molecular orientation in a wide variety of thin films.

## Experimental:

**Sample preparation:** C4FA ( $M_n$ : 4672) was available as a product of C4SFA<sup>®</sup> made by Daikin Industries, Ltd. (Osaka, Japan), and it was used without further purification. A fluorocarbon-soluble solvent, HCFC-225, was purchased from Wako Pure Chemical

Industries, Ltd. (Osaka, Japan). A spin-coated film was prepared on a Si substrate from the HCFC-225 solution ( $9.56 \text{ mg mL}^{-1}$ ) at 8000 rpm on an ACTIVE (Saitama, Japan) ACT-300D spin coater. The substrate having the size of  $40 \times 20 \times 1 \text{ mm}^3$  was purchased from Pier Optics (Gunma, Japan). The film thickness was ca. 50 nm, which was revealed by X-ray reflectivity measurements performed on a Rigaku (Tokyo, Japan) SuperLab X-ray diffractometer.

**IR ATR measurements and calculation procedure:** An IR ATR spectrum of a bulk sample of C4FA was measured by a Thermo Fischer Scientific (Madison, WI, USA) Magna 550 without a polarizer. The internal reflection element was made of germanium, and the interferogram was accumulated 500 times. The angle of incidence was fixed at  $45^\circ$ . An un-polarized ATR spectrum reflects both  $x$  and  $z$  components of the electric permittivity of the thin film that correspond to the TO and LO functions, respectively (Figure 1).<sup>9</sup> The ideal pMAIRS-IP and -OP spectra are, on the other hand, driven by the pure TO and LO functions, respectively.<sup>8</sup> To predict the ideal pMAIRS spectra, therefore, the ATR spectrum is needed to be converted to the TO and LO functions. The spectral conversion of an ATR spectrum to TO and LO functions was performed as follows.<sup>17,18,20</sup> When the ATR spectrum is converted by using the KK relationship considering the angle of incidence, the  $\alpha$  spectrum is obtained where  $\alpha = 4\pi n''/\lambda$  and

$n = n' + in''$  (complex refractive index). The  $\alpha$  spectrum is converted again by the KK relationship considering the angle of incidence to generate  $n'$ ,<sup>20</sup> and the complex relative electric permittivity,  $\varepsilon_r = n^2$ , is obtained on an assumption that  $\varepsilon_{r,\infty}$  is estimated to be  $n_\infty^2$ . For C4FA,  $n_\infty = 1.35$  was conveniently employed.<sup>17,18</sup> Then, both TO and LO energy-loss functions are readily obtained as  $\text{Im}(\varepsilon_x)$  and  $\text{Im}(-1/\varepsilon_z)$ , respectively.<sup>17,18</sup>

The band position is discussed in the accuracy of  $0.1 \text{ cm}^{-1}$ . Since the wavenumber resolution is set to  $4 \text{ cm}^{-1}$ , however, a spectrum is recorded by  $2 \text{ cm}^{-1}$ , which implies that “peak-top position” cannot directly be used for discussing the band position. Instead, the “center-of-gravity position” of a band is read to be a genuine band position. This reading was repeated at least three times, which exhibited an adequate precision of  $\pm 0.1 \text{ cm}^{-1}$ .

**IR pMAIRS measurements:** IR pMAIRS spectra were obtained by Thermo Fischer Scientific Nicolet 6700 FT-IR equipped with Thermo Fischer Scientific (Yokohama, Japan) automatic MAIRS equipment (TN10-1500). Details of the measurement are referred to literature.<sup>21</sup> In the present work, the refractive index of the substrate and the angles of incidence are parameters for optimizing the angle set. For a comprehensive study, 41 single-beam spectra were measured at the angles of incidence varied from  $5^\circ$

to  $45^\circ$  by  $1^\circ$  steps, with which pMAIRS spectra were calculated<sup>5</sup> by choosing an angle set. The accumulation number is 256. In this paper, some representative results are selectively presented. The substrates of Ge ( $n = 4.0$ ), Si ( $n = 3.41$ ), ZnSe ( $n = 2.4$ ) and  $\text{CaF}_2$  ( $n = 1.4$ ) with the size of  $40 \times 20 \times 1 \text{ mm}^3$  were analyzed as representative IR-transparent materials, which were all purchased from Pier Optics.

## Results and Discussion:

**Benefit of using pMAIRS instead of MAIRS:** Before discussing the optimization, the superiority of pMAIRS to the original MAIRS is mentioned first. Figure 2 presents two collections of single beam spectra measured with an angle set (from  $10^\circ$  to  $45^\circ$  by  $7^\circ$  steps) using un-polarized (a) and p-polarized IR rays (b). As found in Figure 2a, the intensity of single beam spectra increases, and the spacing between the adjacent two spectra is monotonously broadening with an increase of the angle of incidence. This pattern shows that the MAIRS measurements are correctly performed.<sup>5</sup> On closer inspection, however, a part of the spectra are nearly overlapped below ca.  $1100 \text{ cm}^{-1}$  on the change of the angle. This is the reason why the original MAIRS has a lowest analytical limit down to ca.  $1100 \text{ cm}^{-1}$ .

On the other hand, the overlapping is significantly improved by using the p-polarized ray (Figure 2b). The spacing between the adjacent two spectra is adequately

kept large through a wide angle range, which covers  $800\text{ cm}^{-1}$  or less. In fact, the pMAIRS technique works well even in the low-wavenumber region down to ca.  $700\text{ cm}^{-1}$ .<sup>21</sup> Therefore, in the present study, the experimental optimization is performed only for pMAIRS.

**Optimization of pMAIRS:** Figure 3 presents a raw IR ATR spectrum of a bulk sample of C4FA in a finger print region. The region is mainly of the C–F stretching vibration bands. The most intense band at  $1133\text{ cm}^{-1}$  is particularly assigned to the symmetric  $\text{CF}_2$  stretching vibration ( $\nu_s(\text{CF}_2)$ ) mode on the perfluoroalkyl chain.<sup>17,18,22</sup> Another strong band at  $1221\text{ cm}^{-1}$  is difficult to be assigned because of heavy overlap of many bands.<sup>18</sup> The band intensity of the  $\nu_s(\text{CF}_2)$  mode is very strong when compared even with that of the  $\nu(\text{C=O})$  mode ( $1740\text{ cm}^{-1}$ ). A strongly absorbing band like the  $\nu_s(\text{CF}_2)$  band is known to exhibit Berreman’s effect, which induces the TO-LO splitting. Since the TO and LO functions correspond to the pMAIRS-IP and OP spectra, respectively, the theoretically predicted TO and LO spectra must be reproduced by the pMAIRS spectra, if the experiments are performed on the optimal condition. In this paper, the predicted spectra from the ATR spectra are named “ATR-TO and -LO” spectra.

Figure 4 presents the IR ATR-TO and -LO spectra of the bulk C4FA sample. As expected, apparent band shifts are found between the two spectra: the  $\nu_s(\text{CF}_2)$  band in



the ATR-LO spectrum is apparently higher shifted by  $4.5\text{ cm}^{-1}$  than that in the ATR-TO one (see inset). This significant shift is a result of the TO-LO splitting. In a similar manner, another strong band of the  $\nu(\text{C}=\text{O})$  mode is found to exhibit an apparent TO-LO splitting ( $4.0\text{ cm}^{-1}$ ). Here, the  $\nu_s(\text{CF}_2)$  mode is chosen as the standard band for optimizing the experimental condition for pMAIRS. This is because the  $\nu(\text{C}=\text{O})$  band is overlaid by the water vapor peaks widely distributed in  $1900\text{--}1300\text{ cm}^{-1}$ , while the  $\nu_s(\text{CF}_2)$  band is not disturbed by these peaks.

Figures 5 and 6 present the IR pMAIRS-IP and -OP spectra of a C4FA spin-coated film deposited on a Si substrate, which are obtained by using various ‘angle sets’ summarized in Table 1 (2nd column). As found in Figure 5, the IP spectra are impervious to the angle set, and they are almost identical to the ATR-TO spectrum in Figure 4. In this manner, the IP spectrum is driven by the pure TO energy-loss function spectrum only, which is free from the choice of the angle set.<sup>8</sup> On the other hand, the OP spectrum responds to the choice of angle set (Figure 6): the bands with a strong absorption coefficient, such as the  $\nu_s(\text{CF}_2)$  and  $\nu(\text{C}=\text{O})$  modes, are highly shifted as the ending angle is large (see inset). Therefore, a comprehensive study of the angle set is definitely needed for obtaining a reliable OP spectrum especially for a strongly absorbing band.

Table 1 shows the band position of the  $\nu_s(\text{CF}_2)$  mode in the IR ATR-LO spectrum and that in the pMAIRS-OP spectrum on Si as a function of the angle set. As found in the table, the band position has a strong correlation with the angle set, particularly for the ending angle: the band is shifted to a lower-wavenumber when the ending angle is small. For example, the angle set from  $6^\circ$  to  $31^\circ$  ( $6^\circ\text{--}31^\circ$ ) yields the band at  $1135.7\text{ cm}^{-1}$  that is between the ATR-TO and the ATR-LO bands, which indicates that the OP spectrum involves not only the LO function component, but also the TO one. This is the reason why the OP spectrum becomes inaccurate. On the other hand, when the ending angle of incidence is larger than  $43^\circ$ , the band position of the OP spectrum ( $1137.8\text{--}1138.4\text{ cm}^{-1}$ ) is fairly closed to that in the ATR-LO spectrum at  $1138.2\text{ cm}^{-1}$ . In particular, when the angle set is taken as  $9^\circ\text{--}44^\circ$ , the band position agrees with that predicted by the ATR-LO spectrum (see the column of  $\nu_{\text{OP}} - \nu_{\text{LO}}$ ). In this manner, the angle set of  $9^\circ\text{--}44^\circ$  is suggested to be the optimal condition for pMAIRS on Si.

Not only the peak position, but the entire spectral shape of the pMAIRS-OP spectrum obtained by the optimal angle set ( $9^\circ\text{--}44^\circ$ ) is also nearly identical to the ATR-LO one (Figure 4) as presented in Figure 7. Note that the  $\nu(\text{C=O})$  band in the OP spectrum presents at  $1744.8\text{ cm}^{-1}$  is also accurately predicted by the ATR-LO spectrum

(1744.6  $\text{cm}^{-1}$ ). This clearly indicates that the OP spectrum on the optimal angle set is purely composed of the LO function, excluding the TO one. In this manner, a new calibration method using the wavenumber shift on Berreman's effect has been accomplished.

To examine the analytical accuracy in the ordinate scale, the molecular orientation in a thin film of highly oriented molecules is checked. To do that, a self-assembled monolayer (SAM)<sup>23,24</sup> of octadecyl trimethoxy silane (ODS)<sup>25</sup> prepared on a Si substrate is employed. The IR pMAIRS spectra of the SAM measured by using the optimal angle set are presented in Figure 8. The  $\text{CH}_2$  stretching vibration ( $\nu(\text{CH}_2)$ ) modes, which appear in 3000–2800  $\text{cm}^{-1}$ , are useful for revealing the tilt angle of the alkyl chain. Since the molecular tilt angle in a monolayer of a heptadecyl- or an octadecyl-containing compound has already been known (ca. 25° from the surface normal),<sup>25,26,27</sup> the IP and OP bands of the  $\nu(\text{CH}_2)$  modes were used to calculate the orientation angle in the present SAM ( $\phi$ ; Table 2) to check the accuracy of the ordinate scale. Details of the calculation of the orientation angle are referred to literature.<sup>25</sup>

As presented in Table 2, the angle set of 9°–44° yields a very acceptable tilt angle, which agrees with the conventionally known tilt angle of 25°; whereas the angle set of 10°–45°, which is often used for the original MAIRS, gives a poor result of 12°.

The optimized angle set of  $9^{\circ}$ – $44^{\circ}$  with the angle steps of  $5^{\circ}$  has thus proved to be highly reliable not only for the spectral shape, but also for the band intensity. Due to a similar reason, another set of  $8^{\circ}$ – $43^{\circ}$  can also be acceptable. In fact, the pMAIRS-OP spectra with the two angle sets (Figure 8) yield highly reliable results, which are almost identical to the RA spectrum.<sup>28,29</sup>

Next, the same calibration method is applied to another substrate with a different refractive index. As the practically useful substrates for IR spectroscopy other than Si ( $n = 3.4$ ), three materials of Ge ( $n = 4.0$ ), ZnSe ( $n = 2.4$ ) and CaF<sub>2</sub> ( $n = 1.4$ ) are chosen for the calibration as summarized in Tables 3–5. As already shown in Table 1, the difference of the position of the  $\nu_s(\text{CF}_2)$  band between the observed pMAIRS-OP and the ATR-LO spectra ( $\nu_{\text{OP}} - \nu_{\text{LO}}$ ) is close to zero, if the optimal angle set is chosen.

As a result, the optimal angle set is found to be  $9^{\circ}$ – $44^{\circ}$  or  $8^{\circ}$ – $43^{\circ}$  commonly for Ge and ZnSe as well as Si. This is a very fortunate result that we don't have to switch the angle set for pMAIRS, if the refractive index is 2.4 or larger. Only one exception was CaF<sub>2</sub>. As found in Table 5, the optimal angle set is obtained as  $8^{\circ}$ – $38^{\circ}$  with  $6^{\circ}$  steps, which agrees with a previous study.<sup>5</sup>

**Conclusion:** The optimal experimental conditions for IR pMAIRS are revealed on representative IR transparent substrates by using an isotropic thin film of a

fluoroacrylate having a short Rf sidechain (C4FA), which yields an apparent Berreman's shift. On this totally new approach, the optimal angle set has been systematically and comprehensively explored. The optimal angle set is concluded to be categorized into only two groups in terms of the refractive index of the using substrates: Ge ( $n = 4.0$ ), Si ( $n = 3.4$ ) and ZnSe ( $n = 2.4$ ) substrates needs the optimal angle set is from  $9^\circ$  to  $44^\circ$  by  $5^\circ$  steps while  $\text{CaF}_2$  ( $n = 1.4$ ) needs another set from  $8^\circ$  to  $38^\circ$  by  $6^\circ$  steps. The optimal experimental conditions enable us to quantitatively analyze the molecular orientation in a thin film irrespective of the degree of the crystallinity.

**Acknowledgment:** The X-ray reflectivity measurements were performed at Kobe University by courtesy of Professor Kazuo Eda. This work was financially supported by Grant-in-Aid for Scientific Research (A) (No. 15H02185 (TH)) and Grant-in-Aid for Young Scientists (B) (No. 26810075 (TS)) from Japan Society for the Promotion of Science, for which the authors thanks are due.

## References:

1. T. Hasegawa. "A Novel Measurement Technique of Pure Out-of-Plane Vibrational Modes in Thin Films on a Nonmetallic Material with No Polarizer". J. Phys. Chem. B. 2002. 106(16): 4112-4115.

2. T. Hasegawa. “Quantitative Comparative Techniques of Infrared Spectra of a Thin Film”. In: C. Wang, R.M. Leblanc, editors. Recent Progress in Colloid and Surface Chemistry with Biological Applications: ACS Symposium Series. Washington, DC, USA: ACS, 2015. Pp. 303-327.
3. T. Hasegawa. “A New Spectroscopic Tool for Surface Layer Analysis: Multiple-Angle Incidence Resolution Spectrometry”. Anal. Bioanal. Chem. 2007. 388(1): 7-15.
4. David L. Drapcho, T. Hasegawa. “Applications of Infrared Multiple Angle Incidence Resolution Spectrometry”. Spectroscopy. 2015. 30(8): 31-38.
5. T. Hasegawa. “Advanced Multiple-angle Incidence Resolution Spectrometry for Thin-Layer Analysis on a Low-Refractive-Index Substrate”. Anal. Chem. 2007. 79(12): 4385-4389.
6. T. Hasegawa, L. Matsumoto, S. Kitamura, S. Amino, S. Katabe, J. Nishijo. “Optimum Condition of Fourier Transform Infrared Multiple-Angle Incidence Resolution Spectrometry for Surface Analysis”. Anal. Chem. 2002. 74(23): 6049-6054.

7. T. Hasegawa, Y. Itoh, A. Kasuya. “Experimental Optimization of p-Polarized MAIR Spectrometry Performed on a Fourier Transform Infrared Spectrometer”. *Anal. Sci.* 2008. 24(1): 105-109.
8. Y. Itoh, A. Kasuya, T. Hasegawa. “Analytical Understanding of Multiple-Angle Incidence Resolution Spectrometry Based on a Classical Electromagnetic Theory”. *J. Phys. Chem. A.* 2009. 113(27): 7810–7817.
9. V.P. Tolstoy, I.V. Chernyshova, V.A. Skryshevsky. “Handbook of Infrared Spectroscopy of Ultrathin Films”. Chichester, UK: John Wiley, 2003. Pp. XX-XX.
10. J. Umemura, T. Kamata, T. Kawai, T. Takenaka. “Quantitative Evaluation of Molecular Orientation in Thin Langmuir-Blodgett Films by FT-IR Transmission and Reflection-absorption Spectroscopy”. *J. Phys. Chem.* 1990. 94(1): 62-67.
11. H.-B. Liu, S.-J. Xiao, Y.-Q. Chen, J. Chao, J. Wang, Y. Wang, Y. Pan, X.-Z. You, Z.-Z. Gu. “Grazing Angle Mirror-Backed Reflection (GMBR) for Infrared Analysis of Monolayers on Silicon”. *J. Phys. Chem. B.* 2006. 110(36): 17702-17705.
12. Y. Nagao. “Highly Oriented Sulfonic Acid Groups in a Nafion Thin Film on Si Substrate”. *J. Phys. Chem. C.* 2013. 117(7): 3294-3297.
13. Y. Nagao. “Proton Transport Property of Nafion Thin Films on MgO(100) with Anisotropic Molecular Structure”. *e-J. Surf. Sci. Nanotech.* 2012. 10: 114-116.

14. D.W. Berreman. “Infrared Absorption at Longitudinal Optic Frequency in Cubic Crystal Films”. *Phys. Rev.* 1963. 130(6): 2193-2198.
15. K. Yamamoto, H. Ishida. “Optical Theory Applied to Infrared Spectroscopy”. *Vib. Spectrosc.* 1994. 8(1): 1-36.
16. K. Yamamoto, A. Masui. “TO-LO Splitting in Infrared Spectra of Thin Films”. *Appl. Spectrosc.* 1996. 50(6): 759-763.
17. T. Hasegawa, T. Shimoaka, N. Shioya, K. Morita, M. Sonoyama, T. Takagi, T. Kanamori. “Stratified Dipole-Arrays Model Accounting for Bulk Properties Specific to Perfluoroalkyl Compounds”. *ChemPlusChem.* 2014. 79(10): 1421-1425.
18. T. Hasegawa, T. Shimoaka, Y. Tanaka, N. Shioya, K. Morita, M. Sonoyama, H. Amii, T. Takagi, T. Kanamori. “An Origin of Complicated Infrared Spectra of Perfluoroalkyl Compounds Involving a Normal Alkyl Group”. *Chem. Lett.* 2015. 44(6): 834-836.
19. K. Honda, M. Morita, H. Otsuka, A. Takahara. “Molecular Aggregation Structure and Surface Properties of Poly(fluoroalkyl acrylate) Thin Films”. *Macromolecules.* 2005. 38(13): 5699-5705.



20. J. Plaskett, P. Schatz. “On the Robinson and Price (Kramers-Kronig) Method of Interpreting Reflection Data Taken through a Transparent Window”. J. Chem. Phys. 1963. 38(3): 612-617.
21. N. Shioya, T. Shimoaka, K. Eda, T. Hasegawa. “A New Schematic for Poly (3-alkylthiophene) in an Amorphous Film Studied Using a Novel Structural Index in Infrared Spectroscopy”. Phys. Chem. Chem. Phys. 2015. 17(20): 13472-13479.
22. C.J. Peacock, P.J. Hendra, H.A. Willis, M.E.A. Cudby. “Raman spectrum and vibrational assignment for poly (tetrafluoroethylene)”. J. Chem. Soc. A. 1970. 2943-2947.
23. J. Sagiv. “Organized Monolayers by Adsorption. 1. Formation and Structure of Oleophobic Mixed Monolayers on Solid Surfaces”. J. Am. Chem. Soc. 1980. 102(1): 92-98.
24. R. Maoz, J. Sagiv. “On the Formation and Structure of Self-Assembling Monolayers. I. A Comparative ATR-Wettability Study of Langmuir-Blodgett and Adsorbed Films on Flat Substrates and Glass Microbeads”. J. Colloid Interface Sci. 1984. 100(2): 465-496.

25. S. Norimoto, S. Morimine, T. Shimoaka, T. Hasegawa. “Analysis of the Surface Coverage of a Self-Assembled Monolayer of Octadecyl Silane on a Si(100) Surface by Infrared External-Reflection Spectroscopy”. *Anal. Sci.* 2013. 29(10): 979-984.
26. T. Hasegawa, Y. Nakano, Y. Ishii. “Molecular Orientation Analysis of a Single-monolayer Langmuir-Blodgett Film on a Thin Glass Plate by Infrared Multiple-angle Incidence Resolution Spectrometry”. *Anal. Chem.* 2006. 78(6): 1739-1742.
27. T. Takenaka, K. Nogami, H. Gotoh, R. Gotoh. “Studies on Built-Up Films by Means of the Polarized Infrared ATR Spectrum I.: Built-Up Films of Stearic Acid”. *J. Colloid Interface Sci.* 1971. 35(3): 395-402.
28. J. Gun, R. Iscovici, J. Sagiv. “On the Formation and Structure of Self-Assembling Monolayers II. A Comparative Study of Langmuir-Blodgett and Adsorbed Films Using Ellipsometry and IR Reflection-Absorption Spectroscopy”. *J. Colloid Interface Sci.* 1984. 101(1): 201-213.
29. M.D. Porter, T.B. Bright, D.L. Allara, C.E.D. Chidsey. “Spontaneously Organized Molecular Assemblies. 4. Structural Characterization of *n*-Alkyl Thiol Monolayers on Gold by Optical Ellipsometry, Infrared Spectroscopy, and Electrochemistry”. *J. Am. Chem. Soc.* 1987. 109(12): 3559-3568.

### Figure captions:

- Figure 1 Interrelationship between the representative infrared spectroscopic techniques via the corresponding energy-loss functions.
- Figure 2 Single-beam spectra at various angles of incidence by  $7^\circ$  steps measured on a Si substrate using an IR un-polarized (a) and a p-polarized rays (b).
- Figure 3 An IR ATR spectrum of a bulk sample of C4FA.
- Figure 4 TO (red) and LO (blue) energy-loss function spectra of a bulk sample of C4FA calculated from the IR ATR spectrum in Figure 3 using  $n = 1.35$ . The absorbance is normalized using the  $\nu_s(\text{CF}_2)$  band at ca.  $1135 \text{ cm}^{-1}$  to be compared to the IR pMAIRS spectra of a thin film of C4FA in Figures 5 and 6.
- Figure 5 IR pMAIRS-IP spectra of a thin film of C4FA measured by using various angle set. The inset shows magnified spectra of the  $\nu_s(\text{CF}_2)$  wavenumber region.
- Figure 6 IR pMAIRS-OP spectra of a thin film of C4FA measured by using various angle set. The inset shows magnified spectra of the  $\nu_s(\text{CF}_2)$  wavenumber region.
- Figure 7 IR pMAIRS spectra of a thin film of C4FA measured with the optimal angle set from  $9^\circ$  to  $44^\circ$  by  $5^\circ$  steps.

Figure 8 IR pMAIRS spectra of a SAM of ODS measured by using three different angle sets of  $8^{\circ}$ – $43^{\circ}$ ,  $9^{\circ}$ – $44^{\circ}$ , and  $10^{\circ}$ – $45^{\circ}$  with  $5^{\circ}$  steps.

Table 1 The position of the  $\nu_s(\text{CF}_2)$  band in the IR pMAIRS-OP spectrum of a C4FA thin film deposited on a Si substrate, and the ATR-LO spectrum of a bulk solid of C4FA as a function of the angle set.

	Angles set and step	$\nu_s(\text{CF}_2) / \text{cm}^{-1}$	$\nu_{\text{OP}} - \nu_{\text{LO}} / \text{cm}^{-1}$
pMAIRS-OP	$6^\circ - 31^\circ; 5^\circ$	1135.7	-2.5
	$7^\circ - 32^\circ; 5^\circ$	1136.2	-2.0
	$8^\circ - 33^\circ; 5^\circ$	1136.2	-2.0
	$9^\circ - 34^\circ; 5^\circ$	1136.4	-1.8
	$10^\circ - 35^\circ; 5^\circ$	1136.4	-1.8
	$6^\circ - 36^\circ; 6^\circ$	1136.4	-1.8
	$7^\circ - 37^\circ; 6^\circ$	1136.6	-1.6
	$8^\circ - 38^\circ; 6^\circ$	1137.0	-1.2
	$9^\circ - 39^\circ; 6^\circ$	1137.2	-1.0
	$10^\circ - 40^\circ; 6^\circ$	1137.4	-0.8
	$6^\circ - 41^\circ; 5^\circ$	1137.3	-0.9
	$7^\circ - 42^\circ; 5^\circ$	1137.6	-0.6
	$8^\circ - 43^\circ; 5^\circ$	1137.8	-0.4
	$9^\circ - 44^\circ; 5^\circ$	1138.2	0
	$10^\circ - 45^\circ; 5^\circ$	1138.4	+0.2
ATR-LO	$45^\circ$	1138.2	—

Table 2 Molecular orientation angle in SAM calculated from the dichroic ratio of the pMAIRS-IP and OP spectra.

Sample	Angle set and step	Orientation angle ( $\phi$ ) / °
SAM	8° – 43°; 5°	28
	9° – 44°; 5°	25
	10° – 45°; 5°	12
Stearic acid <sup>26</sup>	–	25

Table 3 The position of the  $\nu_s(\text{CF}_2)$  band in the IR pMAIRS-OP spectrum of a C4FA thin film deposited on a Ge substrate, and the ATR-LO spectrum of a bulk solid of C4FA as a function of the angle set.

	Angle set and step	$\nu_s(\text{CF}_2) / \text{cm}^{-1}$	$\nu_{\text{OP}} - \nu_{\text{LO}} / \text{cm}^{-1}$
pMAIRS-OP	$6^\circ - 41^\circ; 5^\circ$	1137.7	-0.5
	$7^\circ - 42^\circ; 5^\circ$	1137.7	-0.5
	$8^\circ - 43^\circ; 5^\circ$	1138.1	-0.1
	$9^\circ - 44^\circ; 5^\circ$	1138.4	+0.2
	$10^\circ - 45^\circ; 5^\circ$	1138.8	+0.6
ATR-LO	$45^\circ$	1138.2	—

Table 4 The position of the  $\nu_s(\text{CF}_2)$  band in the IR pMAIRS-OP spectrum of a C4FA thin film deposited on a ZnSe substrate, and the ATR-LO spectrum of a bulk solid of C4FA as a function of the angle set.

	Angle set and step	$\nu_s(\text{CF}_2) / \text{cm}^{-1}$	$\nu_{\text{OP}} - \nu_{\text{LO}} / \text{cm}^{-1}$
pMAIRS-OP	$6^\circ - 41^\circ; 5^\circ$	1137.2	-1.0
	$7^\circ - 42^\circ; 5^\circ$	1137.4	-0.8
	$8^\circ - 43^\circ; 5^\circ$	1137.8	-0.4
	$9^\circ - 44^\circ; 5^\circ$	1138.5	+0.3
	$10^\circ - 45^\circ; 5^\circ$	1138.8	+0.6
ATR-LO	$45^\circ$	1138.2	—



Table 5 The position of the  $\nu_s(\text{CF}_2)$  band in the IR pMAIRS-OP spectrum of a C4FA thin film deposited on a  $\text{CaF}_2$  substrate, and the ATR-LO spectrum of a bulk solid of C4FA as a function of the angle set.

	Angle set and step	$\nu_s(\text{CF}_2) / \text{cm}^{-1}$	$\nu_{\text{OP}} - \nu_{\text{LO}} / \text{cm}^{-1}$
pMAIRS-OP	$6^\circ - 36^\circ; 6^\circ$	1137.3	-0.9
	$7^\circ - 37^\circ; 6^\circ$	1137.6	-0.6
	$8^\circ - 38^\circ; 6^\circ$	1138.3	+0.1
	$9^\circ - 39^\circ; 6^\circ$	1138.7	+0.5
	$10^\circ - 40^\circ; 6^\circ$	1139.3	+1.1
ATR-LO	$45^\circ$	1138.2	—

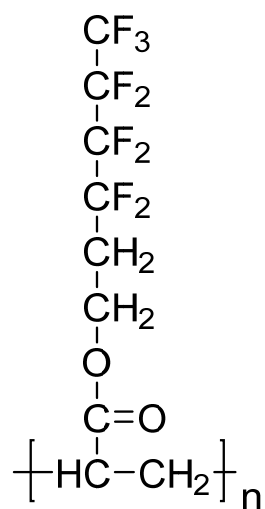


Chart 1 Chemical structure of poly(2-perfluorooctylethyl acrylate), C4FA.

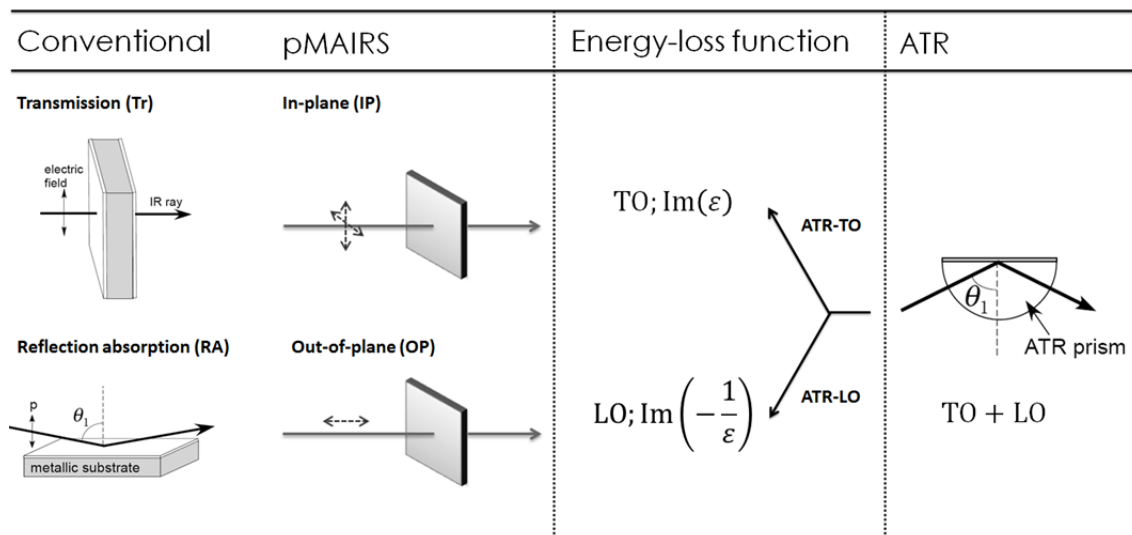


Figure 1 N. Shioya et al.

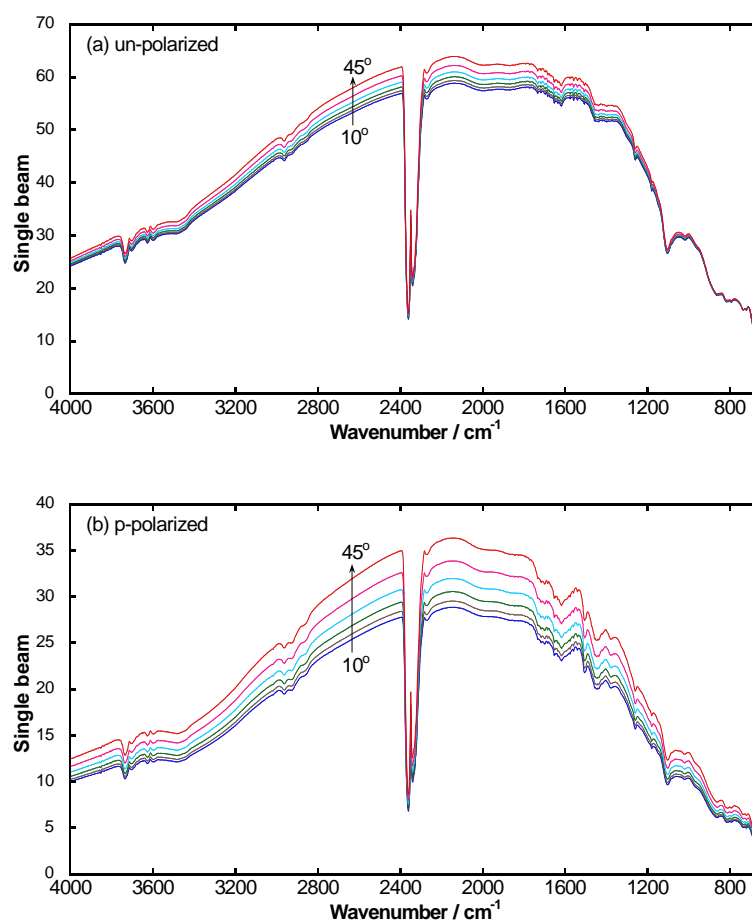


Figure 2 N. Shioya et al.

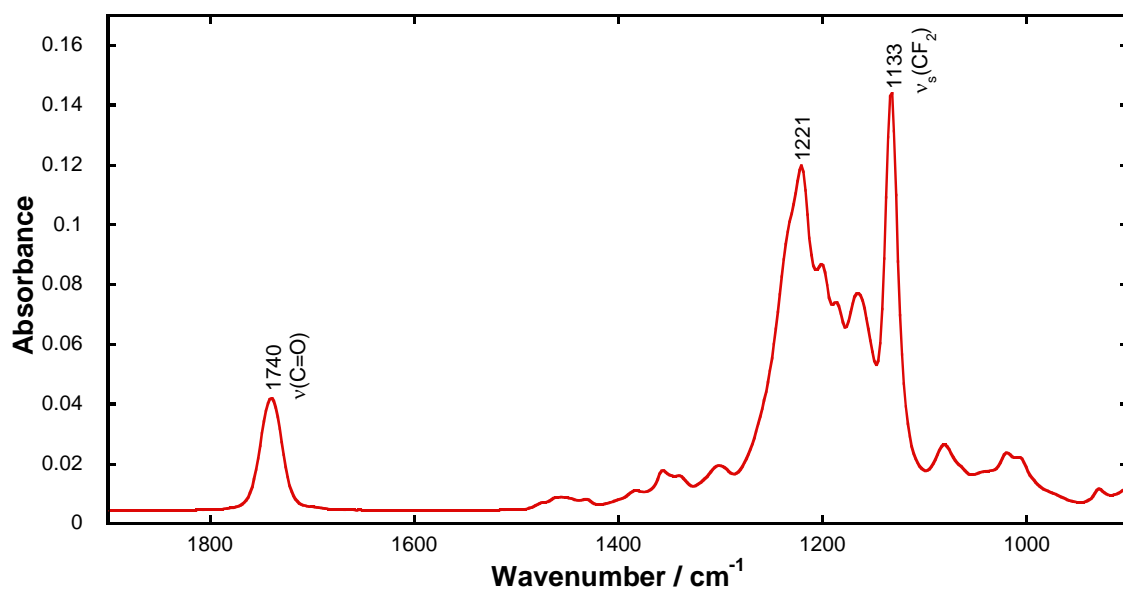


Figure 3 N. Shioya et al.

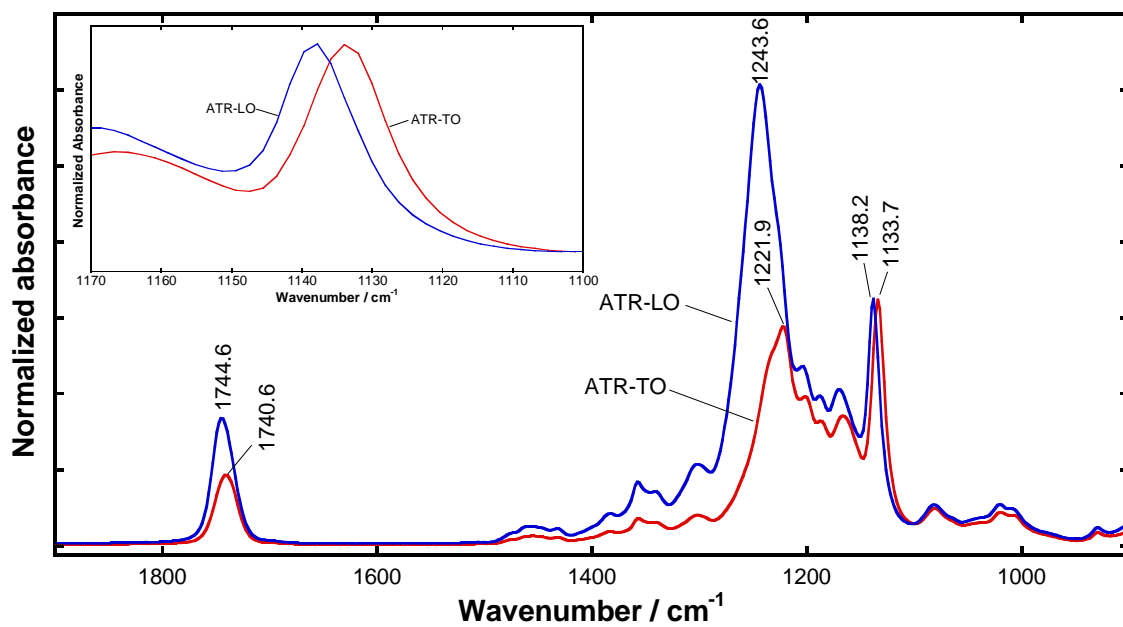


Figure 4 N. Shioya et al.

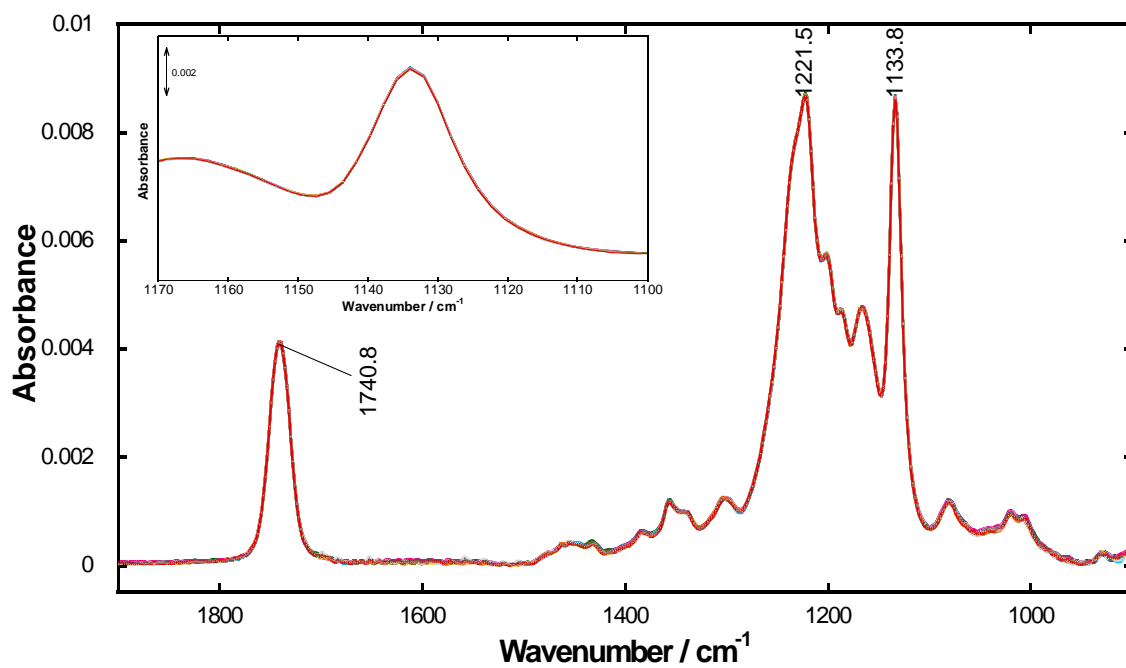


Figure 5 N. Shioya et al.

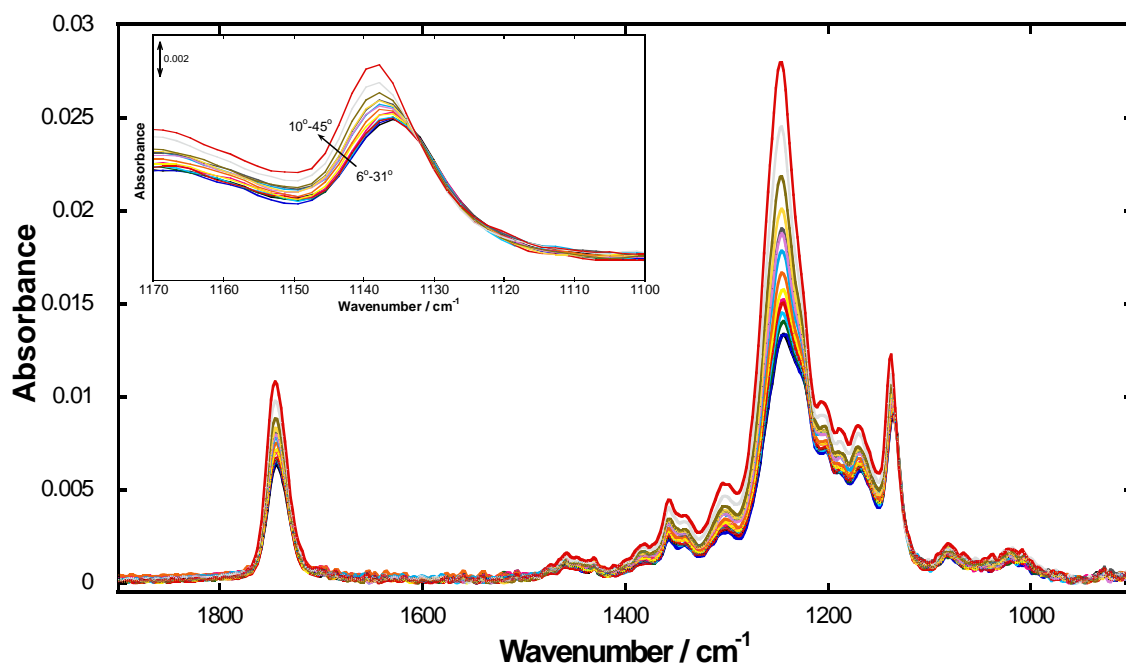


Figure 6 N. Shioya et al.



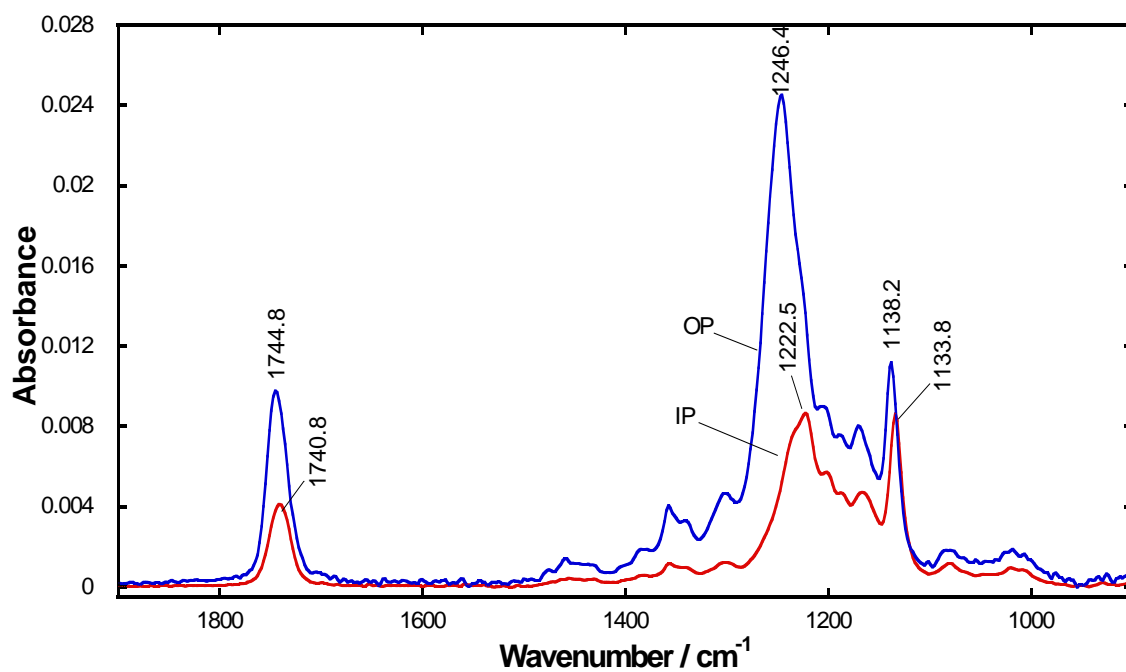


Figure 7 N. Shioya et al.

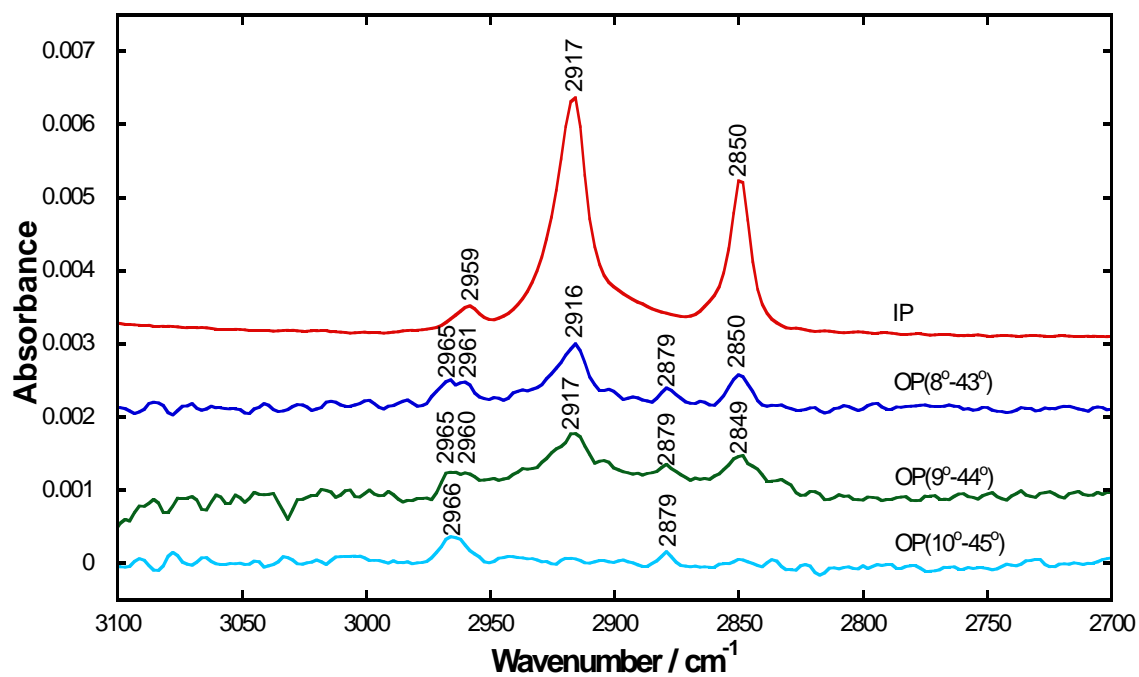


Figure 8 N. Shioya et al.